Tactile simulation of textile fabrics: Design of simulation signals with regard to fingerprint

Benjamin Weiland, Floriane Leclinche, Anis Kaci, Brigitte Camillieri, Betty Lemaire-Semail, Marie-Ange Bueno

Tactile Simulation of Textile Fabrics: Design of Simulation Signals with Regard to Fingerprint

Benjamin Weiland[1], Floriane Leclinche[1], Anis Kaci[2], Brigitte Camillieri[1], Betty Lemaire-Semail[2], Marie-Ange Bueno[1]

[1] Université de Haute-Alsace, Laboratoire de Physique et Mécanique Textiles (LPMT, UR 4365), École Nationale Supérieure d'Ingénieurs Sud-Alsace, F-68093 Mulhouse Cedex, France (benjamin.weiland@uha.fr; floriane.leclinche@uha.fr; brigitte.camillieri@uha.fr; marie-ange.bueno@uha.fr)

[2] Univ. Lille, Arts et Metiers Institute of Technology, Centrale Lille, Junia, ULR 2697 - L2EP, F-59000 Lille, France (anis.kaci@univ-lille.fr; betty.semail@polytech-lille.fr).

Corresponding author: Floriane Leclinche (floriane.leclinche@uha.fr)

Abstract:

This study describes a systematic approach to generate control signals of a tactile simulator to render the touch of textile fabrics. As a friction modulation tactile surface is used, control signals were generated from tribological measurements on real surfaces. Forces were acquired from an artificial finger, with a texture mimicking fingerprints. Then the signals are processed in frequency domain and send as control signal to the tactile stimulator. This paper focusses on the potential benefits of including the fingerprint information in the simulation of fabrics for achieving realistic tactile perception. A sensory analysis with 36 participants was carried out using the generated control signals, and results show a better discrimination without fingerprint information.

Index Terms:

Tribology, textile fabrics, fingerprint, surface textures, tactile, friction control, tactile simulator

1. Introduction

Tactile simulation of real textures is of significant interest for materials in object design: B2C (business to consumer) [1] or B2B (business to business) e-commerce of products and in particular textile materials in direct interaction with humans (garments, furnishing, seat or wall covers for home or transport, etc.). Indeed, such simulation could allow virtual prototyping as a design aid and reduce the product development time and the number of samples to produce while also simplifying the interactions necessary for the development and therefore reducing the environmental impact.

To this end, the tactile rendering should be efficient, i.e. sufficiently close to real surfaces, and the designer or the manufacturer should be able to easily simulate the surfaces, i.e. should be able to build or complete its own tactile database. Therefore, the process used to build the database, i.e. to add a control signal for the given tactile simulator, should be systematic, from the real surface characterization to the control signal, and without any interaction with a human as a tactile sensor. This needs a specific protocol to be established, independently from the human, but according to the choice of the tactile simulator.

Several methods are reported in the literature for real texture tactile simulation in terms of i) the method used to obtain the input information, ii) the input information used for the control signal, iii) the signal process used to transform the input information into a control signal, iv) the principle of the tactile stimulator and v) the range of the simulated textures. Moreover, the simulation can be purely tactile or multimodal, i.e. with visual and/or audio [2], [3], and thermal stimulation [4]. In the present study the stimulation is purely tactile.

The control signal of the tactile simulator may be acquired by a probe held by a human hand [5], [6], or by the finger used as a probe [7]–[9]. In another way, the control signal can be partially generated by a probe and partially from the finger [10]. Therefore, in all these configurations, the control signal is influenced by the human hand/finger which makes it difficult to identify surface features that are interesting for texture recognition/classification [11]. It may also be deduced only by using a measurement device [11].

The tactile information used to define the control signal can be the roughness profile [3], [12], [13], the acceleration between the probe or the finger and the surface, i.e. friction-induced vibrations [5], [8], [9] or both friction force and acceleration [6]. It can also be visual information from a picture which is converted into a friction signal [14].

From the acceleration, the whole signal can be considered [8], [9], or only an extraction of criteria adapted from audio recognition [11] or using deep learning [2]. The friction properties can also be used, particularly the mean coefficient of friction of the surfaces [7], or its evolution along the surface [4], [15]. Other studies use the evolution of the resulting force calculated from friction and normal forces [16] or the highest harmonic of the friction force due to texture [10], [17].

The simulators used can be a haptic stylus held in the hand [2], [4], [6], [11], which could also be the same device as for the initial signal acquisition [2], [4], [11]. In that case the simulation includes acceleration but also friction and normal forces [4]. The tactile stimulator can be a small area touched by the finger without any movement [8], [9] simulating the acceleration, i.e. friction-induced vibrations. It can also be a pad with an array of vibrating pins [3], [12], [13] simulating a roughness profile, or a continuous plate simulating friction by using friction modulation, due to electro-adhesion [7], [14] or ultrasonic vibrations [10].

The simulated textures can come from a wide range of materials such as paper, polymer, stone, wood, textile surfaces, etc. [2], [4], [6], [11]–[13], or in a more reduced space composed by polymer [8], [9] or textile surfaces [7], [10], [14]. Of course, for the simulation into a same cluster of materials, the

information included in the control signal must be more accurate than for wide clusters. Indeed, in the first case, the goal is to accurately discriminate surfaces close to each other in comparison to the second case. Textile fabric texture is very specific because it can present a superficial hairiness which is very difficult to characterize in terms of roughness. This hairiness can have a main direction, such as for velvet, therefore the surface property is anisotropic [10], [16]. In addition, the hairs are dense, i.e. several hundred per square centimetre, and need a good resolution for the simulation. Therefore, pin-array stimulators seem inappropriate for this purpose, whereas continuous surface stimulators are better candidates. This explains why the studies considering a wide range of textile surfaces used the friction modulation principle [7], [10], [14].

The tactile stimulator chosen here, called the STIMTAC, is based on friction modulation due to ultrasonic vibrations [18] because it has a good spatial resolution, approximately 100 µm, for a sufficiently large active surface, which in its current form is approximately 70x50 mm^2, but larger plates are available. Moreover, this device has already provided encouraging results for textile surface simulation [10]. However, the control signal was partially generated by a combination of two friction signals: one from an artificial finger and the other from a real finger; therefore, the procedure was not entirely systematic. With this aim, the method used to obtain the tactile information necessary to design the control signal should be independent from a particular finger. The strategy adopted here is to use an artificial finger previously developed [23], including a texture representing the fingerprint or dermatoglyphs, as an "average" finger, to acquire the friction data resulting from the surface interaction.

Several studies proved the presence of an interaction between dermatoglyphs and the texture of the explored surface [19], [20], specifically with textile structures [21], [22] and in particular with hairiness [23]. This interaction is included in the tactile information obtained from the artificial finger used. On the other hand, the perception of the simulated texture from the tactile simulator is the result of the interaction between the surface of the simulator and the finger of the user, with his/her own fingerprints. However, as

the simulator surface is without any texture (at the scale of interest), this interaction results in a weak stimulation of the user dermatoglyphs. Therefore, in order to simulate a texture, and specifically a textile surface, should the information from the interaction with the dermatoglyphs be included in the control signal or not? The goal of this study is to answer this question.

In the present paper, in the first part the wide range of real textile fabrics investigated and the tribological experiments are presented, then the systematic signal processing used to generate the virtual fabrics is described. Then, the two experiments used for the sensory analysis to compare real and virtual fabrics are described. In the second part, the results are shown, highlighting the similarities and differences between simulations, with or without taking into account dermatoglyphs, and real surfaces for a wide range of textile fabrics. Lastly, the discussion gives an analysis and explanation of these similarities and differences.

2. Material and methods

2.1. Real fabrics investigated

For this study, five textile fabrics have been selected as they represent a wide range for the clothing industry and a wide range of surface states (Table I).

The main characteristics of these fabrics are presented below:

- A Pekin woven cotton fabric which presents very distinct bumps in the warp direction (Fig. 1 a),
- A twill cotton fabric (Fig. 1 b),
- A plain woven cotton fabric (Fig. 1 c),
- A knitted velvet made from two yarns: a ground yarn forming the knit structure (in polyester polyethylene terephthalate - PET) and a plush yarn (in wool) appearing only on one side (Fig. 1 d). For this fabric, the pile has a preferred direction called “along-pile” in which piles lie down and the opposite direction is called “against-pile”. These two directions will be tested in this study and are considered as two different fabrics (R4 and R5 Table I).

- A knitted polar fleece made from two polyester yarns (PET): a ground yarn forming the knit structure and a yarn forming loops on one side of this structure (Fig. 1 e). After knitting, a raising process allows the creation of tangled hairs on the two fabric faces. The number of patterns for this fabric cannot be determined because it is hidden by the hairiness.

From these 5 real fabrics, a total of 6 sample fabrics are considered.

Differences in surface hairiness can be observed: fabrics with little or no hair, such as plain woven (Fig. 1 f), Pekin or twill fabrics have a similar profile, while fabrics such as velvet or fleece are very hairy, as shown in Fig. 1 g) and h). Moreover, as fabrics are made by interlacing threads, a number of patterns per cm can define them.

TABLE I: Fabric characteristics

Ref.	Fabrics	Raw material	Patterns/cm
R1	Pekin	100% cotton	7
R2	Twill	100% cotton	8.5
R3	Plain woven	100% cotton	24
R4	Velvet against pile	80% wool 20% PET	11.5
R5	Velvet along pile		
R6	Polar fleece	100% PET	/

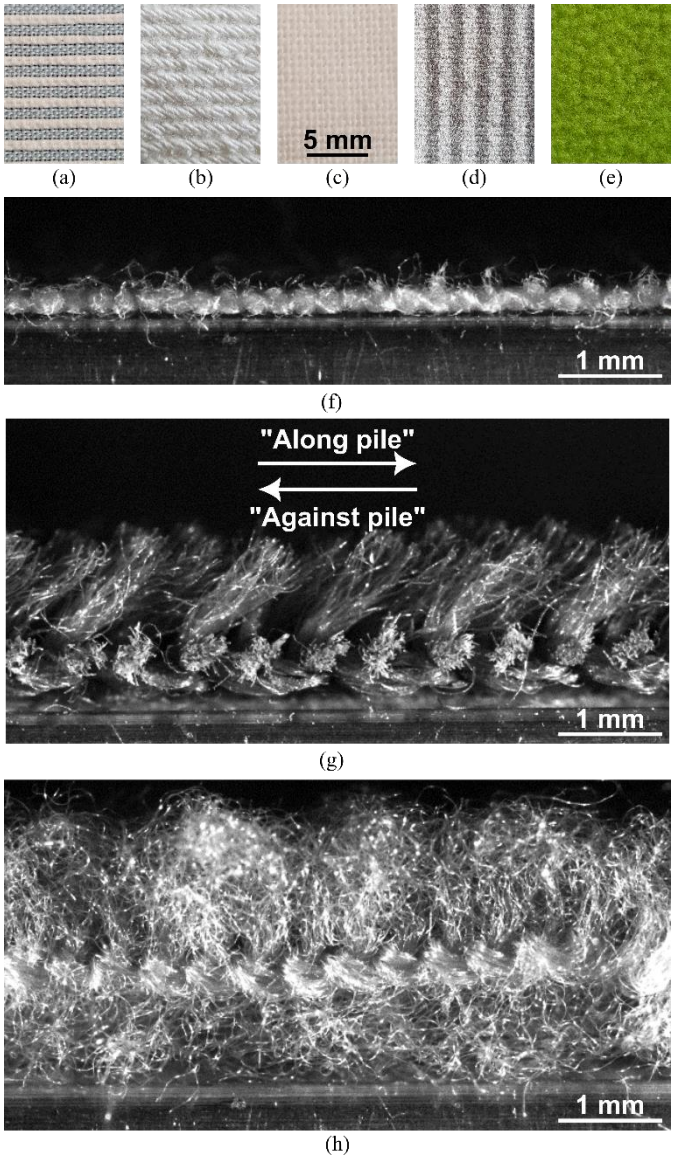

Fig. 1. Images of fabrics: (a) Pekin, (b) cotton twill, (c) plain woven, (d) velvet and (e) polar fleece. Fabric profile of (f) plain woven, (g) velvet and (h) polar fleece.

2.2. Tribological measurements

2.2.1. Tribometer description

Real fabric tactile information was obtained from a tribometer (Fig. 4) described in a previous paper [1]. It allowed the study of reciprocating linear motion with a pin on plane contact. A slider was rubbed against

the fabrics placed on a translation table driven by a magnetic brushless linear motor (*ILS300LM-S*, Newport, controlled by an *XPS-RLDM, Motion Controller*, Newport). The slider was linked to the frame thanks to a strain-gauge sensor (*HBM PW4C3 sensor*, HBM France SAS, Mennecy, France, acquired through a *signal conditioning amplifier 2210A*, Vishay Measurement Group, Raleigh, North Carolina) which allowed the measurement of the friction force F_t. Another force sensor (*K1107-20N*, Scaime, acquired through a conditioner rail *ME520-AJ*, Doerler Measures) was used to measure the normal contact force F_n. Data acquisition was achieved thanks to a Pulse data recorder (*Controller Module Tupe 7536*, Brüel & Kjaer, Mennecy, France). The macro-tribometer was used with an imposed height configuration where the slider was fixed at a given height during a test. The height was adjustable and was chosen to impose the desired normal force.

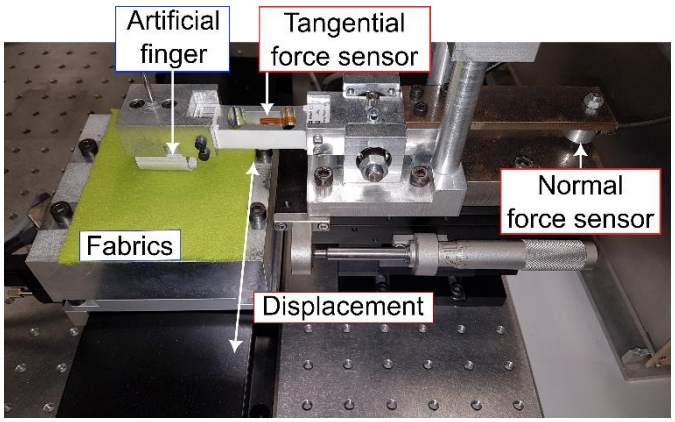

Fig. 4. Macro-tribometer.

2.2.2. Artificial finger

An artificial finger developed in a previous study [23] was used as the slider to represent a mean human finger in contact with textile surfaces. It is composed of a silicone slider covered by a textured fabric (Fig. 5) with a spatial period SP_f = 536 ± 9 µm and a roughness Rt = 95 ± 8 µm [23]. This fabric was selected because its characteristics are similar to the dermatoglyphs of human fingers, [26]–[28] and the resulting

COF (2) between the artificial finger and the fabric was close to that between real fingers and fabrics [23]. However, the artificial finger presents another main period SP_w, resulting from the weaving pattern of the textured fabric, which does not correspond to the finger characteristics.

$$COF = \frac{F_t}{F_n} \quad (2)$$

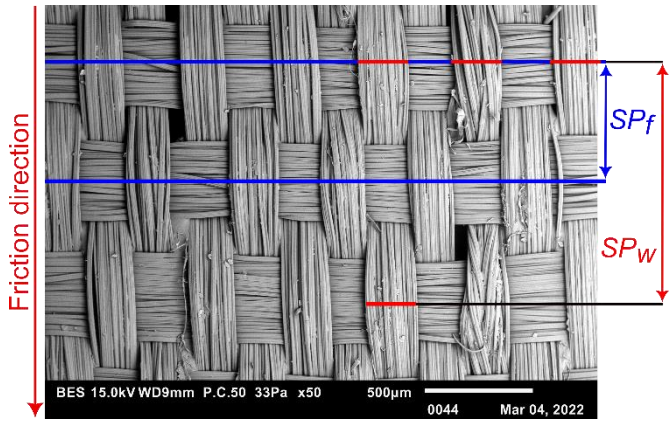

Fig. 5. Textured fabric covering the silicone slider. SP_f is the spatial period representing the fingerprint and SP_w the spatial period due to the weaving pattern. Measured with a scanning electron microscope (SEM, Jeol JSM-IT 100).

2.3. Virtual fabric generation

2.3.1. Tactile simulator: STIMTAC

The textile fabrics were simulated using a tactile device called the STIMTAC (Fig. 2), which is described in detail in a previous work [16]. The operating principle of this device is based on the reduction of the

coefficient of friction (COF) by ultrasonic lubrication. The vibration frequency of the STIMTAC is between 30-40 kHz, which is too high to be perceived by the human finger, which cannot perceive vibrations at frequencies above 1 kHz [24], [25]. These vibrations are generated by excitations of piezoelectric ceramics placed under a plate in beryllium coated with a vinyl polymer film (*Ra* = 1.23 µm). Friction is reduced by the intermittent contact which occurs between the fingertip and the vibrating surface as well as the layer of air trapped between the plate and the fingertip. The COF is lowest at the maximum vibration amplitude, i.e. approximately 2 µm. To simulate textures, the vibration amplitude is controlled as a function of the finger position on the active surface. A supply signal length of *Ns* = 1024 is needed while the STIMTAC values corresponding to the vibration amplitude are coded on an octet.

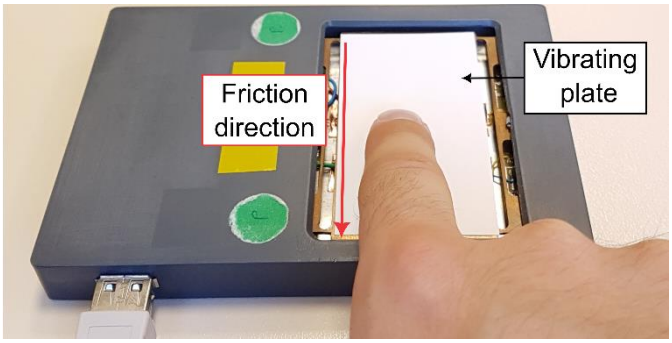

Fig. 2. STIMTAC.

Some preliminary friction tests were carried out with the tribometer, presented in section 2.2, to validate STIMTAC capacities to simulate multiple textures frequencies from 10 to 50 Hz, including 1 to 4 frequencies (1_f to 4_f) in the supply signals (1). $\boldsymbol{A}$ corresponds to the vibration amplitude, x the position on the STIMTAC, f_i the frequency added to $\boldsymbol{A}$. A very good correspondence between the command and experimental frequencies obtained from STIMTAC has been verified (Fig. 3).

$$\boldsymbol{A}(x) = \sum_{i=1}^{i=1:4} \sin(2\pi f_i x) \quad (1)$$

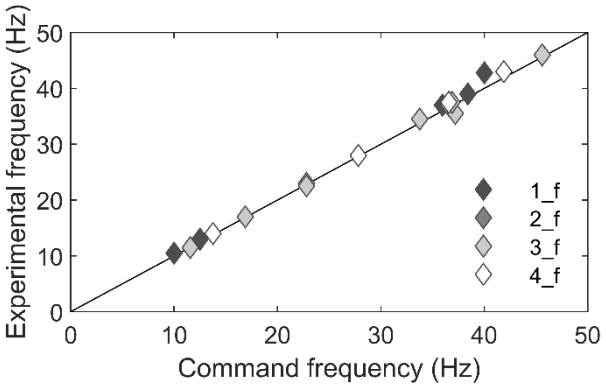

Fig. 3. Experimental frequencies simulated relative to the STIMTAC command frequencies. Measurements were performed with the macro-tribometer presented below at a speed of 20 mm.s^{-1} and a normal force of 0.5 N.

2.3.2. Virtual fabric generation by systematic signal processing

Step 1: Signal acquisition

As presented in section 2.2., tribological measurements were used to obtained the information from the friction interaction between the real fabrics investigated and the artificial finger. The friction tests were conducted at a velocity of 20 mm.s^{-1} over a sliding distance of 70 mm and a desired normal force of 0.5 N. For each fabric, 8 to 12 samples were used with 15 cycles per sample. Thus, both forces F_t and F_n were obtained as a function of time at a sampling frequency of 8192 Hz (Fig. 6 – Step 1).

From the complete time signals of both forces $\boldsymbol{F_t}$ and $\boldsymbol{F_n}$, a 3.2 s time window where the motion speed is constant was kept for each half cycle, in both directions to obtained the reduced time signals $\boldsymbol{F_i(t)}$ ($\boldsymbol{F_i}$ = $\boldsymbol{F_t}$ *or* $\boldsymbol{F_n}$). An exception was made for the velvet, for which both directions lead to a clear difference in friction behaviour and perceptions. Therefore, for this fabric, each direction was treated as a separate sample and

was measured with its own set of parameters to ensure a normal force close to the target. Thus, in this particular work, the transition signal was not analysed.

Step 2: Forces spectra

Park et al. [29] have shown with a sensory experiment that the Discrete Fourier Transform was the best method to reduce a 3-axis acceleration signal to a 1-axis vibration signal to transcribe the perception. The following signal processing step was inspired from the same method.

The signal processing was performed using Matlab. The reduced time signals $\boldsymbol{F_i}(t)$ ($\boldsymbol{F_i}$ = $\boldsymbol{F_t}$ *or* $\boldsymbol{F_n}$) were considered in the frequency domain from a Fast Fourier Transform (FFT).

Algorithm 1 summarizes the operations used to calculate the mean spectrum of both forces $\overline{\boldsymbol{F_t}(f)}$ and $\overline{\boldsymbol{F_n}(f)}$ (Fig. 6 – Step 2). For visibility, all spectra are displayed with logarithm scales, and the frequency range is shown from 10 to 320 Hz. The weighting window $\boldsymbol{W}$ used is a Planck-Taper type (ε = 0.1035). f is the frequency and t the time. $\overline{F_i(t)}$ is the average of one time window data points and $\overline{\boldsymbol{F_i}(f)}$ is the average of the FFT obtained for all of the fabric samples. The frequency spectrum resolution is Δf = 0.3125 Hz.

Algorithm 1 Signal processing: Step 2 (Matlab)

$$\boldsymbol{F_i}(f) = \text{abs}\left(\text{fft}\left(\boldsymbol{W}.*\left(\boldsymbol{F_i}(t) - \overline{F_i(t)}\right)\right)\right)$$

$$\overline{\boldsymbol{F_i}(f)} = \text{mean}\left(\boldsymbol{F_i}(f)\right)$$

Step 3: Resulting force

As determined in [16], the resulting force which combines friction and normal forces has been previously considered as an interesting variable to incorporate into the control signal the information of hardness or, more precisely, the finger penetration in thickness directions in soft fabrics. In fact, when the finger penetrates into hairy surfaces, both tangential and normal force vary during tactile movement.

The resulting force spectrum $\boldsymbol{F}(f)$ was calculated (3) for each fabric (Fig. 6 – Step 3). Peaks were visible on these spectra and some of them were artifacts that do not contain useful information for the contact finger/fabric. It was therefore necessary to clean up the peaks of each spectrum.

$$\boldsymbol{F}(f) = \sqrt{\overline{\boldsymbol{F_t}(f)}^2 + \overline{\boldsymbol{F_n}(f)}^2} \qquad (3)$$

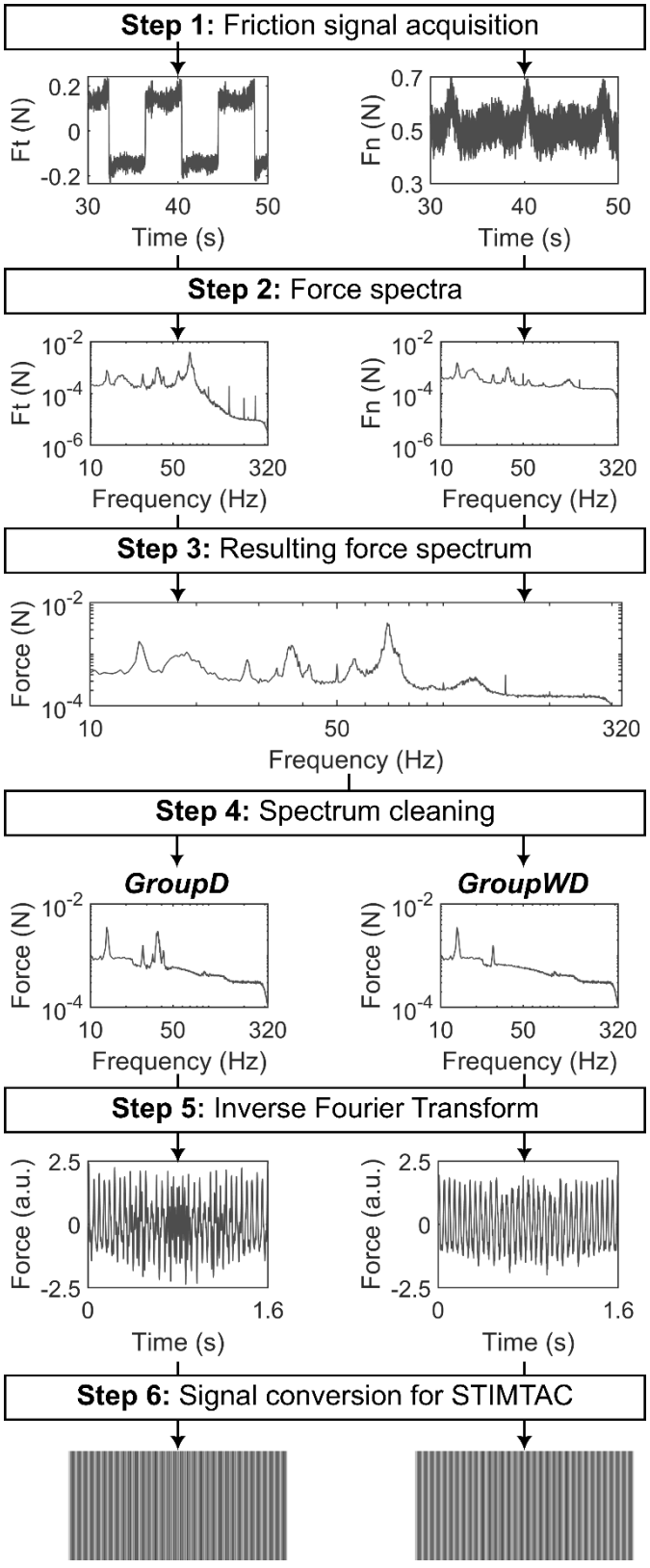
Step 1: Friction signal acquisition
Ft (N)
0.2
0
-0.2
30
40
50
Time (s)
Fn (N)
0.7
0.5
0.3
30
40
50
Time (s)
Step 2: Force spectra
Ft (N)
10-2
10-4
10-6
10
50
320
Frequency (Hz)
Fn (N)
10-2
10-4
10-6
10
50
320
Frequency (Hz)
Step 3: Resulting force spectrum
Force (N)
10-2
10-4
10
50
320
Frequency (Hz)
Step 4: Spectrum cleaning
GroupD
Force (N)
10-2
10-4
10
50
320
Frequency (Hz)
GroupWD
Force (N)
10-2
10-4
10
50
320
Frequency (Hz)
Step 5: Inverse Fourier Transform
Force (a.u.)
2.5
0
-2.5
0
1.6
Time (s)
Force (a.u.)
2.5
0
-2.5
0
1.6
Time (s)
Step 6: Signal conversion for STIMTAC

Fig. 6. Different steps of the signal processing used to generate the virtual fabrics from the friction acquisition signals between the artificial finger and a fabric (here with the example of Pekin).

Step 4: Peak identification and spectrum cleaning

The unnecessary peaks were removed and replaced by a baseline.

The following peaks could be identified and were cleaned:

- The *ac power supply* leads to multiple fine peaks, at 50 Hz and harmonics.
- The *continuous parts* from both forces (0 to 10 Hz) are not exploitable due to the very high values of these bandwidth on the spectra.
- The macro-tribometer is mainly responsible of one peak (70 Hz), which does not depend on the motion speed. It corresponds to the resonance frequency of the tangential force sensor, as proven by shock tests.
- The fabric covering the artificial finger has a second period SP_w. As indicated previously, this period does not correspond to the finger characteristics, but it leads to a peak and its third harmonic. These peaks were thus cleaned.

At the end, for each fabric, two virtual samples were generated (Fig. 6 – Step 4) (see section 2.4):

- ***GroupD***: samples with dermatoglyph information (SP_f), containing also the textile peaks and the baseline.
- ***GroupWD***: samples without dermatoglyph information (SP_f), containing only the textile peaks and the baseline.

Step 5: Inverse Fourier transform

The next step is to use an Inverse Fast Fourier Transform (IFFT) to generate a time signal for the resulting force $\boldsymbol{F}(t)$ following (4), and using the weighting window $\boldsymbol{W}$ (Fig. 6 – step 5).

$$\boldsymbol{F}(t) = \left(\text{IFFT}\left(N.* \boldsymbol{F}(f)\right)\right)./\boldsymbol{W} \qquad (4)$$

Step 6: Signal conversion to command STIMTAC

Algorithm 2 summarizes the processing. The first operation aims to convert the temporal signal $\boldsymbol{F}(t)$ into a spatial signal $\boldsymbol{F}(x)$, relative to *x*, the finger position on the STIMTAC. As we consider a given exploration speed of 20 mm.s^{-1}, this was done thanks to a constant factor a = 0.64, allowing to generate the wanted frequencies on the STIMTAC. Finally, the desired signal length (N_s) was kept.

The conversion between force values and the STIMTAC input values is made using two parameters, depending on the fabrics used in the study.

The friction contrast (*FC*) [10] was used to adjust the average friction coefficient on the tactile device thanks to the STIMTAC mean level (*Mlv*) of the vibration amplitude. *L* is a constant used to adapt the signal $\boldsymbol{F}(t)$ to the STIMTAC. In this study, the polar fleece is the fabric with the highest COF. $\boldsymbol{COF_{fabrics}}$ and $\boldsymbol{F_{fabrics}}(f)$ represent respectively the coefficients of friction and the signal $\boldsymbol{F}(f)$ of all fabrics used.

The root mean square contrast (RMSC) was used to adjust the signal intensity. The constant $C = 0.45$ was then introduced and enables to fine-tune the virtual fabric intensity which correspond to the peak-to-peak value of the vibration amplitude. Finally, the signals were normalized ($\boldsymbol{F_{Norm}}(x)$) before calculating the STIMTAC supply signals ($\boldsymbol{F_{STIMTAC}}(x)$) used to generate the virtual samples (Fig. 6 – step 6).

Algorithm 2 Signal processing: Step 6 (Matlab)

Conversion to a spatial signal

$$\boldsymbol{F}(x) = \text{resample}(\boldsymbol{F}(t), Ns, Ns/a))$$

Friction contrast

$$FC = 1 - COF/\,max\left(\boldsymbol{COF}_{\boldsymbol{fabrics}}\right)$$

$$Mlv = L(1 + FC)$$

RMS contrast

$$RMSmax = \max\left(\text{rms}\left(\boldsymbol{F}_{\boldsymbol{fabrics}}(f)\right)\right)$$

$$RMSC = 1 + C.\ln\left(\text{rms}\left(\boldsymbol{F}(f)\right)/RMSmax\right)$$

Conversion to command the STIMTAC

$$Range = \max\left(\boldsymbol{F}(x)\right) - \min\left(\boldsymbol{F}(x)\right)$$

$$\boldsymbol{F}_{\boldsymbol{Norm}}(x) = L\left(2.\frac{\left(\boldsymbol{F}(x) - \min\left(\boldsymbol{F}(x)\right)\right)}{Range} - 1\right)$$

$$\boldsymbol{F}_{\boldsymbol{STIMTAC}}(x) = Mlv + RMSC * \boldsymbol{F}_{\boldsymbol{Norm}}(x)$$

2.4. Sensory analysis: Participants, tasks and data processing

All the experiments were carried out in accordance with the 1964 Helsinki declaration and its subsequent amendments or comparable ethical standards. Informed consent was obtained from all individual participants included in the study.

This aims of the experiment were to verify if:

- the virtual fabrics correctly transcribed the perception of the real fabrics,
- the artificial finger main period SP_f, representing the finger dermathoglyphs, has to be included in the control signal to generate a realistic sensory perception on the STIMTAC.

2.4.1. Experiment 1: Confusion matrix

To this end, an experiment where participants had to attribute a virtual fabric to a real one was realized to achieved confusion matrices, in order to visualize the participants' capacity to identify the virtual fabrics in both configurations, with or without dermathoglyph information.

At the start of the test, participants were asked to select the finger they wished to use for exploration, usually the index finger of their dominant hand. The required movement was only in the proximal direction, with a required normal force between 0.5 and 1 N and a friction speed of approximately 20 $mm.s^{-1}$. Note that in the case of tactile saturation, participants were allowed to change fingers.

The normal force applied by the participants was controlled on the STIMTAC during the experiment and they had to apply the same force on the real fabrics. It was verified that the participants maintained a stable normal force during the contact, and were able to repeat tests with the same force.

For evaluating the realistic perception of virtual fabrics, thirty-six participants were selected (15 males and 21 females, with an age range of 21 to 64) from different activity sectors (administrative, technical, professor and student). None of them had participated in a similar experiment previously.

Each participant was requested to follow the same experimental procedure during approximately 30 minutes. The experiment took place in a room whose atmosphere was conditioned (20 ±2°C and 65 ± 5% of relative humidity). This procedure was chronologically organized as follows:

- The participant washed and dried his/her hands;
- As in other studies [26], [30], skin hydration was measured using a Corneometer® CM825. To normalize the results, this device was mounted on a homemade system, enabling the same force (4.9 N) to be applied for each measurement. The Corneometer is described by Fluhr *et al*. [31]. Ten measurements were taken for each participant before the perception tests because the finger skin hydration can have a considerable influence on friction and therefore on tactile perception [26], [32];
- A training session was performed on real fabrics and on virtual textures, different from those used in the experiment. This session was done in order to explain the protocol to the participants and enable them to become familiar with the STIMTAC surface;
- The participants were separated in two groups: *GroupD* tested the virtual fabrics with the dermatoglyphs and *GroupWD* conducted tests without this information. In order to ensure the same homogeneity in both groups, we paid a particular attention to participant skin hydration to allocate them. Indeed, skin hydration plays an important role in friction contrast on the STIMTAC by increasing the COF values and limiting the perception of small stimulation intensity variation [26], [33]. Thus, it was important to obtain similar distributions regarding skin hydration in both groups.

Firstly, participants had access to the STIMTAC and real fabrics, these being hidden from view in a box. A virtual fabric was presented to participants who then had to select the real sample they thought corresponded to the simulation. To avoid perceptual bias, participants wore noise-cancelling headphones,

the real samples were hidden from view and the order of presentation was random. For each participant, a confusion matrix can be determined. These matrices are then combined to form a global confusion matrix.

To establish the confusion matrix, the 6 real samples (Ri) are presented in columns and the virtual samples in rows (Di or WDi depending on the group). Each virtual fabric was presented twice during the session. For example, the virtual fabrics obtained with the Pekin (R1), named D1 if containing the dermatoglyphs information or WD1 if not, were proposed twice. If the participant associates this simulation with the real R1 fabric in both occurrences, the value 2 will be entered in the matrix on the diagonal. If he/she associates it once with R1 and once with R2 for instance, the value will be 1 for each fabric.
For the results to be convincing, a well-marked diagonal would have to be found, indicating each simulation was associated with its corresponding fabric.
By definition, when a confusion matrix is presented, the references, i.e. the real fabrics in this study, must be classified by proximity. For that purpose, a sensory analysis was performed to classify the fabrics.

2.4.2. Experiment 2: Intensity ratings

In this context, twenty-six participants were selected (14 males and 12 females, with an age range of 24 to 56) from different activity sectors. After some training and assessment of their performance according to the sensory method used in the literature [34], 11 panellists were selected from the group. The selection was performed according to their highest repeatability in the sensory analysis. Note that this study was carried out with French terms, here translated for the needs of publication but with the inevitable minor changes due to the cultural specificities associated with a language.

To characterize the surface of real fabrics, three sensory attributes were chosen: two binary and one single. Two were taken from the four main psycho-perceptive dimensions that were smooth/rough, slippery, soft/hard and cold/hot [35]–[38]. As two of them were not relevant to the STIMTAC, a hedonic attribute was added. The chosen attributes are the following:

- Smooth/Rough (*Rp*)
- Slippery (*Gp*)
- Unpleasant/Pleasant (*Pp*)

The movement of the finger for the perception assessment was the same as previously. For each descriptor, panellists were asked to rate their intensity using an unstructured linear scale from 0 to 100. The average was calculated over 4 sessions. To avoid perceptual bias, participants wore noise-cancelling headphones and the samples were hidden from view. In addition, to avoid any memory effect from one session to the next, both the samples and attribute evaluations were presented in a random order. Skin hydration was measured before and after the perception assessment.

In order to classify the fabrics for the confusion matrices, a Principal Component Analysis (PCA) was performed. PCA allows us to simplify the structure of data while preserving as much information as possible. With the PCA, a set of correlated variables is transformed into a new set of uncorrelated variables called principal components. This can be useful for understanding and visualizing data, or for classification. This statistical method therefore makes it possible to simplify data and extract the essential information.

3. Results

3.1. Tribological measurements

The friction tests were realized with a normal force of 0.47 ± 0.08 N for all real fabrics. Fig. 7 shows the boxplot of the COF.

It was shown in a previous work [23] the friction behaviour between a real finger and fabrics without oriented pile (such as plain woven fabric and polar fleece) was the same in both directions, while for oriented-pile fabrics, such as velvet, the behaviour differs with the friction direction (along or against pile). The same behaviour was observed in this work, so only the velvet was analysed in both directions. Moreover, the COFs obtained here are very close to those between the fabrics and real fingers obtained in previous work or by Jiao *et al.* with 120 fabrics [7] as well as by Bertaux *et al.* [39] where authors used an artificial skin.

The velvet (R4 – R5) and polar fleece (R6) present a higher mean COF, which is due to the higher penetration depth of the slider into the fabric thickness. In addition, the COF distribution for the polar fleece is large compared to the other fabrics. These higher instabilities during the friction can be explained by the fabric's pile.

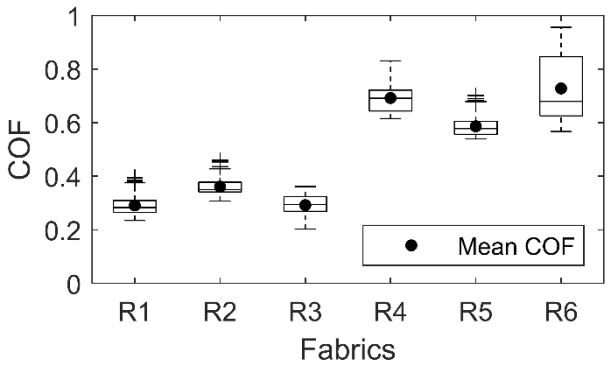

Fig. 7. Boxplot of the coefficient of friction acquired for each real fabric against the artificial finger with the macro-tribometer. The mean COF is added to the boxplot.

Fig. 8 presents the resulting force *F* spectra calculated for all fabrics and for both virtual sample groups *D* and *WD*. As in previous graphs, spectra are displayed with logarithmic scales and a frequency *f* range between 10 and 320 Hz.

The artificial finger peak (SP_f) at 37 Hz is present for all fabrics but differs in bandwidth and intensity. The fabrics with a strong woven pattern such as Pekin (R1), twill (R2) and plain woven (R3) present a higher intensity of this peak than the other three textiles. It can also be seen that the textile peaks are clearly present for all samples excepted for the polar fleece (R6). For this surface, only the baseline and the finger peak seem to exist. This can be explained by the fact that the hairiness of the polar fleece hides the knitting pattern. The textile peaks correspond to the main pattern of the considered fabrics and its harmonics. For velvet, in both directions, a peak appears corresponding to the double value of the structure period. It is assumed that the velvet pile leads to this narrow peak.

Fig. 8 highlights a strong response for the samples R1, R2 and R3, the three other sample peaks are very weak compared to their baseline. Finally, there is two samples for which the finger information peak has a higher intensity than the textile peaks: R3 and R6.

3.2. Sensorial analysis

3.2.1. Experiment 1: Confusion matrix

As explained in section 2.4, participants were divided in two groups according to their finger skin hydration. The first group (16 participants) worked on virtual fabrics with the dermatoglyph information (*GroupD*), and the second group (20 participants) on virtual fabrics without the dermatoglyph information (*GroupWD*). As it was expected, the participants skin hydration follows a normal distribution, ensuring their good separation in both groups (Fig. 9).

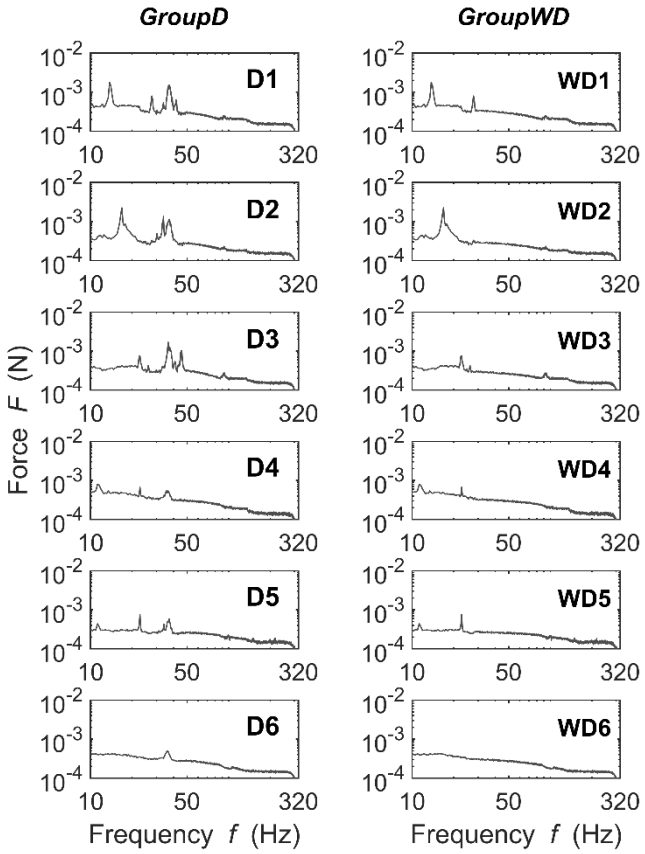

Fig. 8. Spectra obtained from the 6 fabric samples used to generate the virtual fabrics, for both groups of signals: *GroupD* with dermatoglyph information and *GroupWD* without this information.

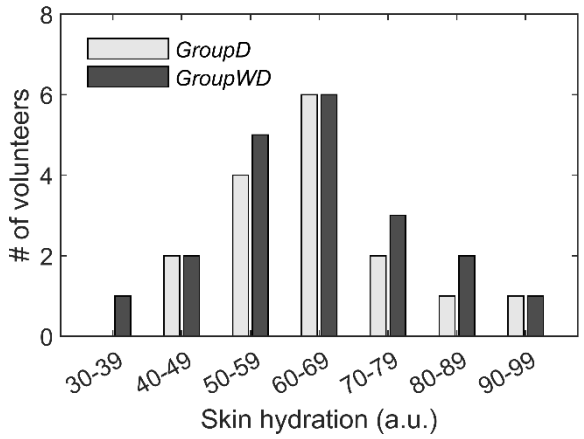

Fig. 9. Distribution of skin hydration for both groups

Once the participants were divided into two groups, they were subjected to sensory tests and their individual confusion matrix was determined. In sensory analysis, a confusion matrix is a tool used to evaluate and analyse the results of sensory evaluation tests. It is used to compare participant sensory evaluations with the reference values for each sample. An example of a matrix is presented Fig. 10.

GroupD #P1	R1	R2	R3	R4	R5	R6
D1			1	1		
D2	1	1				
D3						2
D4		1		1		
D5			1		1	
D6		1	1			

Fig. 10. Example of an individual confusion matrix obtained by participant named #P1. A red cell corresponds to a constant association between real and virtual fabric and a blue cell to a lack of association of the two samples.

Here, the real fabrics were not sorted according to their similarities, which makes reading the results complex. To improve the analysis, the real fabrics were classed.

3.2.2. Experiment 2: Intensity ratings

After the four characterization sessions by the panellists, each real fabric was described according to the three sensory attributes with their own intensity of perception (Table II). It can be noticed skin hydration was measured before and after the experiment. Contacting the fabrics did not seem to change the finger moisture or they regulate it, because globally skin hydration did not change before and after the experiment.

TABLE II: Sensory attributes (*Gp* Slippery, *Rp* Rough and *Pp* Pleasant)

Fabrics	Gp	Rp	Pp
R1: Pekin	28	81	21
R2: Twill	40	71	34
R3: Plain woven	67	37	52
R4: Velvet against pile	19	59	42
R5: Velvet along pile	76	20	79
R6: Polar fleece	75	18	93

Each fabric has its sensory profile. Indeed, the fabrics represent a wide product space for textile materials, resulting in different perceptions of their surface. According to Table II, it was possible to determine groups of fabrics for each attribute (pleasant, slippery or rough). Therefore, based on these data, a Principal Component Analysis (PCA) was performed to visualize the similarities between our samples and group them together. The PCA results are presented in Fig. 11.

The three attributes are closely interrelated, enabling us to identify fabrics and also to batch them (Fig. 11 a). The attribute roughness is strongly correlated with the first PCA axis, with a correlation

coefficient = 0.97. Therefore, two clusters of samples can be easily identified according to their sensory properties and especially their roughness (Fig. 11 b), so R1, R2 and R4 were the roughest ("Rough" cluster) and R3, R5 and R6 were the least rough ("Smooth" cluster) fabrics. These two clusters will be used in the confusion matrices for the remainder of this paper.

During the tests, it was found that perception could vary significantly from one individual to another, whatever the surface explored, real or virtual. Fig. 12 highlights this variability on virtual surfaces for 4 participants. Each of these matrices provides different sensory information on the participant's ability to find the correct sample corresponding to the simulation presented. In order to draw conclusions from these matrices, participant's responses were added together for each fabric cluster according to the PCA (Fig. 12).

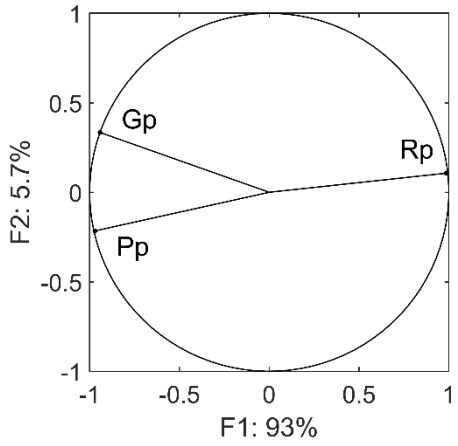

(a)

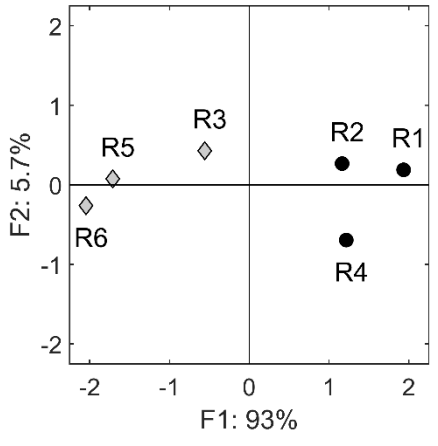

(b)

Fig. 11. Principal Component Analysis on perception data. a) correlation circle between attributes and b) PCA biplot for the two main axes.

4. Discussion

Fig. 12 a) presents the sensory results for a participant who was able to discriminate very well the simulations. Indeed, a diagonal is clearly visible on the matrix, so the participant has succeeded not only in differentiating the simulations but also in associating the corresponding textile samples. In addition, the second matrix (Fig. 12 b) shows the participant's ability to correctly perceive each cluster.

Some of the participants were only able to distinguish both clusters. As shown in Fig. 12 c) which presents the results of a participant who was unable to correctly discriminate each simulation. However, he/she was able to differentiate fabrics into clusters, with the exception of simulations D1 and D6, each of which was recognized once in the wrong one. Thus, the grouped matrix highlights the recognition of D2, D4 as rough fabrics and D3, D5 simulations as smooth ones.

In Fig. 12, the results of matrices e) and f) are very mixed, with clusters confused except for simulations WD3 and WD6, which are correctly recognized. Given the matrices, this participant was not able to perceive correctly the STIMTAC simulations.

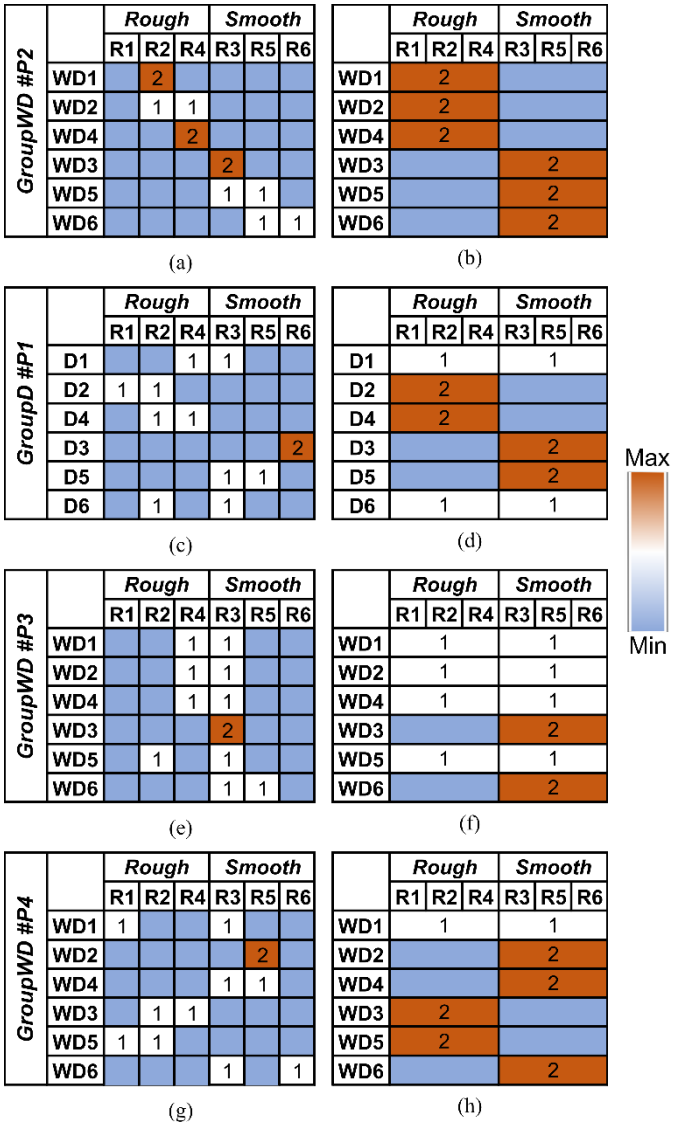

Fig. 12. Examples of individual confusion matrices: for each fabric (left, i.e. a, c, e and g) and by fabric clusters (right, i.e. b, d, f and h).

The last matrices g) and h) present a special case. The participant is able to differentiate between different textures because a diagonal is visible, but in the opposite direction, i.e. simulations WD2, WD4 and WD6 were perceived as smooth fabrics and inversely for the others at the exception of WD1 for which results are mixed. Therefore, it seems that this participant is evaluating textures using a criterion other than roughness.

To answer the question of whether or not dermatoglyphs are of interest in the virtual fabrics, it is interesting to perform an analysis at the scale of global matrices, i.e. the matrices grouping together all the responses of the participants in the study. For this purpose, the individual matrices were summed to determine the overall confusion matrices with and without dermatoglyphs information (Fig. 13 a) and c)). Each matrix is expressed as a percentage. As described previously, the fabrics have been grouped into clusters in the matrices Fig. 13 b) and d) and a colour code indicates whether simulations have been correctly recognized.

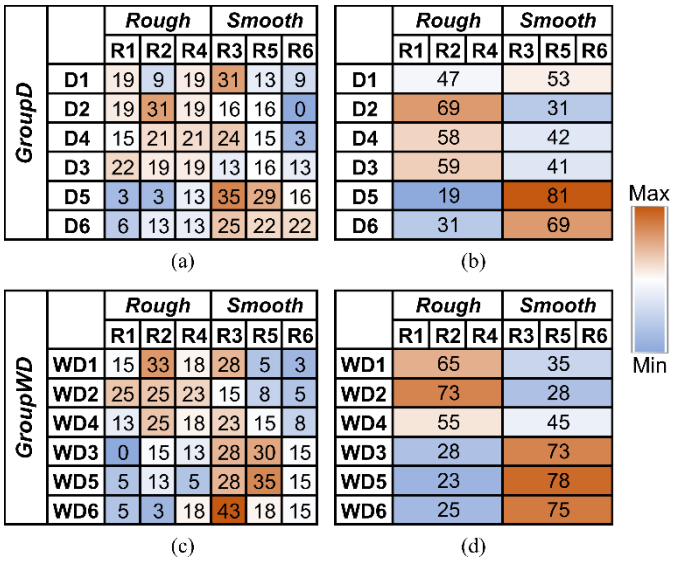

Fig. 13. Global confusion matrices, expressed as a percentage

The global matrix for *GroupD* (Fig. 13 a) shows differences in perception between simulations: some were correctly recognized, like D2, by a large proportion of participants, while others were not recognized at all like D3, D4 or D6 for which no real fabrics were preferably assigned. It can also be noted that among the unrecognized simulations, some were often confused with the same real sample, such as D1, which was associated with R3 for 31% of responses.

For the *GroupWD,* the observations are more or less the same with some differences as for WD6 which was often linked to R3.

By comparing the grouped matrices, a trend emerges between simulations with and without dermatoglyph information, particularly for smooth surfaces. Indeed, the WD3, WD5 and WD6 simulations were recognized as smooth surfaces in more than 70% of cases. For the "*Rough" cluster*, the results are somewhat more mixed. The simulations WD1 and WD2 are well perceived but simulation WD4 is randomly assigned to both clusters, since the response percentages are close to 50%.

As can be seen above in Fig. 8, the finger information used for the *GroupD* virtual samples could contain more energy than the textile information. It is the case for both samples *D3* and *D6*. For *D3*, this high peak can explain why this virtual sample was not attributed to the right cluster ("*Smooth*"), while it was correctly attributed for *WD3*. This was not the case for *D6* as the finger peak is less marked and does not create a strong pattern on the virtual samples. Finally, for Pekin (R1), it seems that the addition of the fingerprint information is hiding the signal patterns, which can explain why WD1 is put in the correct cluster while D1 is not.

Bergmann Tiest *et al.* [40] have tested a wide range of materials: metals, wood, ceramic and some textiles mixed in. They asked volunteers to categorize samples from their similarities, and displayed their data in a PCA. According to their graph, the product space for materials is wide, and textiles represent only a tiny part of it. Within this space, textiles are very close to each other for their roughness and compressibility. Therefore, this observation, plus the one-dimension rendering of the STIMTAC, can explain why it is so difficult for people to discriminate our virtual textile fabrics. Indeed, even if the fabrics considered here presented large differences of tactile perception for the textile product space, some of these differences can be attributed to other dimensions such as the soft/hard and cold/hot criteria, which are not correctly rendered in this experiment.

5. Conclusion

This paper first presents a systematic approach to generate signals to simulate specific surfaces, i.e. textile surfaces. In this approach, the signals were processed from the tangential and normal forces acquired by an artificial finger, with a motion that is similar to a real one, in the proximal direction. The signals measured were filtered to clean the artefacts that were not representative of the contact.

For the virtual fabric simulation, it was possible to add or not add the dermatoglyph information. This was done by keeping or not keeping in the resultant force spectrum the peak due to the artificial finger texture representing dermathoglyphs in terms of spatial period. It is shown that this choice strongly influences the realistic perception of virtual samples. Thus, in this paper, the main goal was to determine which condition was better to ensure a good generation of signals for a realistic perception of textile fabrics.

According to the confusion matrices, the absence of dermatoglyph information in the virtual fabrics seems to be more relevant for surface recognition. This seems to be particularly the case for fabrics where the fingerprint peak is higher than the textile ones, or for textiles for which the patterns will be hidden by the addition of the fingerprint information.

Consequently, fabric clusters are better recognized without dermatoglyphs than with dermatoglyphs, therefore the tactile rendering from tactile device is better in that configuration. To conclude, we suggest to don’t use dermathoglyph information to simulate fabrics. Without dermatoglyphs information the clusters were correctly identified in term of roughness, but they are not individually recognized.

In order to improve individual fabric discrimination, two tracks have been identified: STIMTAC surface coating and control signal design of virtual samples.

The interface between STIMTAC and finger is very sensitive to humidity changes, which is directly related to friction contrast. As such, another STIMTAC coating or texture could reduce the sensitivity to humidity changes and improve results by optimizing the finger/fabric interaction [41].

Regarding the signal processing, the transition between both directions could be studied to generate a more complete virtual fabric. This complement could be used to simulate the finger penetration into hairiness for the polar fleece or the specific change of direction for the velvet.

In addition, several studies have highlighted the value of multisensory stimuli, particularly visual [42], [43], for perception and recognition. Therefore, it would be interesting to carry out a similar study with the real fabrics in plain sight.

Acknowledgment

The authors acknowledge the CNRS-GDR TACT 2033 (Le Toucher: Analyse, Connaissance, simulaTion). We wish to thank Pr. Michel Tourlonias, Sascha Krügl and Christian Pidancier (Université de Haute-Alsace, LPMT, Mulhouse) for manufacturing and installing the macro-tribometer and Corneometer mount. We would also like to thank all the experiment volunteers for participating in this study.

This work was supported in part by Institutes Carnot MICA and ARTS under Grant TacFib, and the French Research Agency (ANR-20-CE28-0010).

References

[1] M. Blazquez Cano, P. Perry, R. Ashman, and K. Waite, “The influence of image interactivity upon user engagement when using mobile touch screens,” *Comput. Hum. Behav.*, vol. 77, pp. 406–412, Dec. 2017, doi: 10.1016/j.chb.2017.03.042.

[2] H. Zheng, L. Fang, M. Ji, M. Strese, Y. Ozer, and E. Steinbach, “Deep Learning for Surface Material Classification Using Haptic and Visual Information,” *IEEE Trans. Multimed.*, vol. 18, no. 12, pp. 2407–2416, Dec. 2016, doi: 10.1109/TMM.2016.2598140.

[3] M. Peruzzini, M. Mengoni, and L. Cavalieri, “A multimodal tactile interface for immersive virtual experience,” *Int. J. Intell. Eng. Inform.*, vol. 5, no. 1, p. 29, 2017, doi: 10.1504/IJIEI.2017.082563.

[4] M. Strese, Y. Boeck, and E. Steinbach, “Content-based surface material retrieval,” in *2017 IEEE World Haptics Conference (WHC)*, Munich, Germany: IEEE, Jun. 2017, pp. 352–357. doi: 10.1109/WHC.2017.7989927.

[5] J. M. Romano, T. Yoshioka, and K. J. Kuchenbecker, “Automatic filter design for synthesis of haptic textures from recorded acceleration data,” in *2010 IEEE International Conference on Robotics and Automation*, Anchorage, AK: IEEE, May 2010, pp. 1815–1821. doi: 10.1109/ROBOT.2010.5509853.

[6] H. Culbertson, J. J. Lopez Delgado, and K. J. Kuchenbecker, “One hundred data-driven haptic texture models and open-source methods for rendering on 3D objects,” in *2014 IEEE Haptics Symposium (HAPTICS)*, Houston, TX, USA: IEEE, Feb. 2014, pp. 319–325. doi: 10.1109/HAPTICS.2014.6775475.

[7] J. Jiao, Y. Zhang, D. Wang, X. Guo, and X. Sun, “HapTex: A Database of Fabric Textures for Surface Tactile Display,” in *2019 IEEE World Haptics Conference (WHC)*, Tokyo, Japan: IEEE, Jul. 2019, pp. 331–336. doi: 10.1109/WHC.2019.8816167.

[8] L. Felicetti, E. Chatelet, A. Latour, P.-H. Cornuault, and F. Massi, “Tactile rendering of textures by an Electro-Active Polymer piezoelectric device: mimicking Friction-Induced Vibrations,” *Biotribology*, vol. 31, p. 100211, Sep. 2022, doi: 10.1016/j.biotri.2022.100211.

[9] L. Felicetti, C. Sutter, E. Chatelet, A. Latour, L. Mouchnino, and F. Massi, “Tactile discrimination of real and simulated isotropic textures by Friction-Induced Vibrations,” *Tribol. Int.*, vol. 184, p. 108443, Jun. 2023, doi: 10.1016/j.triboint.2023.108443.

[10] W. Ben Messaoud, M.-A. Bueno, and B. Lemaire-Semail, “Textile Fabrics’ Texture: From Multi-level Feature Extraction to Tactile Simulation,” in *Haptics: Perception, Devices, Control, and Applications*, F. Bello, H. Kajimoto, and Y. Visell, Eds., in Lecture Notes in Computer Science, vol. 9775. Cham: Springer International Publishing, 2016, pp. 294–303. doi: 10.1007/978-3-319-42324-1_29.

[11] M. Strese, J.-Y. Lee, C. Schuwerk, Q. Han, H.-G. Kim, and E. Steinbach, “A haptic texture database for tool-mediated texture recognition and classification,” in *2014 IEEE International Symposium on Haptic, Audio and Visual Environments and Games (HAVE) Proceedings*, Richardson, TX, USA: IEEE, Oct. 2014, pp. 118–123. doi: 10.1109/HAVE.2014.6954342.

[12] M. Peruzzini, M. Germani, and M. Mengoni, “Electro-tactile device for texture simulation,” in *Proceedings of 2012 IEEE/ASME 8th IEEE/ASME International Conference on Mechatronic and Embedded Systems and Applications*, Suzhou, China: IEEE, Jul. 2012, pp. 178–183. doi: 10.1109/MESA.2012.6275558.

[13] M. Germani, M. Mengoni, and M. Peruzzini, “Electro-tactile device for material texture simulation,” *Int. J. Adv. Manuf. Technol.*, vol. 68, no. 9–12, pp. 2185–2203, Oct. 2013, doi: 10.1007/s00170-013-4832-1.

[14] S. Cai, L. Zhao, Y. Ban, T. Narumi, Y. Liu, and K. Zhu, “GAN-based image-to-friction generation for tactile simulation of fabric material,” *Comput. Graph.*, vol. 102, pp. 460–473, Feb. 2022, doi: 10.1016/j.cag.2021.09.007.

[15] M.-A. Bueno, B. Lemaire-Semail, M. Amberg, and F. Giraud, “A simulation from a tactile device to render the touch of textile fabrics: a preliminary study on velvet,” *Text. Res. J.*, vol. 84, no. 13, pp. 1428–1440, Aug. 2014, doi: 10.1177/0040517514521116.

[16] M.-A. Bueno, B. Lemaire-Semail, M. Amberg, and F. Giraud, “Pile Surface Tactile Simulation: Role of the Slider Shape, Texture Close to Fingerprints, and the Joint Stiffness,” *Tribol. Lett.*, vol. 59, no. 1, p. 25, Jul. 2015, doi: 10.1007/s11249-015-0555-9.

[17] B. Camillieri, M.-A. Bueno, M. Fabre, B. Juan, B. Lemaire-Semail, and L. Mouchnino, “From finger friction and induced vibrations to brain activation: Tactile comparison between real and virtual textile fabrics,” *Tribol. Int.*, vol. 126, pp. 283–296, Oct. 2018, doi: 10.1016/j.triboint.2018.05.031.

[18] M. Biet, F. Giraud, and B. Lemaire-Semail, “Implementation of tactile feedback by modifying the perceived friction,” *Eur. Phys. J. Appl. Phys.*, vol. 43, no. 1, pp. 123–135, Jul. 2008, doi: 10.1051/epjap:2008093.

[19] F. Martinot, “The Influence of Surface Commensurability on Roughness Perception with the Bare Finger,” in *Proc. of Eurohaptics*, Jul. 2006.

[20] R. Fagiani, F. Massi, E. Chatelet, Y. Berthier, and A. Akay, “Tactile perception by friction induced vibrations,” *Tribol. Int.*, vol. 44, no. 10, pp. 1100–1110, Sep. 2011, doi: 10.1016/j.triboint.2011.03.019.

[21] R. Fagiani, F. Massi, E. Chatelet, J. P. Costes, and Y. Berthier, “Contact of a Finger on Rigid Surfaces and Textiles: Friction Coefficient and Induced Vibrations,” *Tribol. Lett.*, vol. 48, no. 2, pp. 145–158, Nov. 2012, doi: 10.1007/s11249-012-0010-0.

[22] V. Massimiani, B. Weiland, E. Chatelet, P.-H. Cornuault, J. Faucheu, and F. Massi, “The role of mechanical stimuli on hedonistic and topographical discrimination of textures,” *Tribol. Int.*, vol. 143, p. 106082, Mar. 2020, doi: 10.1016/j.triboint.2019.106082.

[23] B. Camillieri and M.-A. Bueno, “Artificial finger design for investigating the tactile friction of textile surfaces,” *Tribol. Int.*, vol. 109, pp. 274–284, May 2017, doi: 10.1016/j.triboint.2016.12.013.

[24] J. W. Morley and M. J. Rowe, “Perceived pitch of vibrotactile stimuli: effects of vibration amplitude, and implications for vibration frequency coding.,” *J. Physiol.*, vol. 431, no. 1, pp. 403–416, Dec. 1990, doi: 10.1113/jphysiol.1990.sp018336.

[25] I. Darian-Smith, “The Sense of Touch: Performance and Peripheral Neural Processes,” in *Comprehensive Physiology*, R. Terjung, Ed., 1st ed.Wiley, 1984, pp. 739–788. doi: 10.1002/cphy.cp010317.

[26] P.-H. Cornuault, L. Carpentier, M.-A. Bueno, J.-M. Cote, and G. Monteil, “Influence of physico-chemical, mechanical and morphological fingerpad properties on the frictional distinction of

sticky/slippery surfaces," *J. R. Soc. Interface*, vol. 12, no. 110, p. 20150495, Sep. 2015, doi: 10.1098/rsif.2015.0495.

[27] E. Gutiérrez-Redomero, Á. Sánchez-Andrés, N. Rivaldería, C. Alonso-Rodríguez, J. E. Dipierri, and L. M. Martín, "A comparative study of topological and sex differences in fingerprint ridge density in Argentinian and Spanish population samples," *J. Forensic Leg. Med.*, vol. 20, no. 5, pp. 419–429, Jul. 2013, doi: 10.1016/j.jflm.2012.12.002.

[28] M. A. Acree, "Is there a gender difference in fingerprint ridge density?," *Forensic Sci. Int.*, vol. 102, no. 1, pp. 35–44, May 1999, doi: 10.1016/S0379-0738(99)00037-7.

[29] G. Park and K. J. Kuchenbecker, "Objective and Subjective Assessment of Algorithms for Reducing Three-Axis Vibrations to One-Axis Vibrations," in *2019 IEEE World Haptics Conference (WHC)*, Tokyo, Japan: IEEE, Jul. 2019, pp. 467–472. doi: 10.1109/WHC.2019.8816148.

[30] T. André, V. Lévesque, V. Hayward, P. Lefèvre, and J.-L. Thonnard, "Effect of skin hydration on the dynamics of fingertip gripping contact," *J. R. Soc. Interface*, vol. 8, no. 64, pp. 1574–1583, Nov. 2011, doi: 10.1098/rsif.2011.0086.

[31] J. W. Fluhr, M. Gloor, S. Lazzerini, P. Kleesz, R. Grieshaber, and E. Berardesca, "Comparative study of five instruments measuring stratum corneum hydration (Corneometer CM 820 and CM 825, Skicon 200, Nova DPM 9003, DermaLab). Part I. In vitro," *Skin Res. Technol.*, vol. 5, no. 3, pp. 161–170, Aug. 1999, doi: 10.1111/j.1600-0846.1999.tb00126.x.

[32] M. Arvidsson, L. Ringstad, L. Skedung, K. Duvefelt, and M. W. Rutland, "Feeling fine - the effect of topography and friction on perceived roughness and slipperiness," *Biotribology*, vol. 11, pp. 92–101, Sep. 2017, doi: 10.1016/j.biotri.2017.01.002.

[33] W. B. Messaoud, M.-A. Bueno, and B. Lemaire-Semail, "Relation between human perceived friction and finger friction characteristics," *Tribol. Int.*, vol. 98, pp. 261–269, Jun. 2016, doi: 10.1016/j.triboint.2016.02.031.

[34] G. V. Civille and B. T. Carr, *Sensory Evaluation Techniques*, 0 ed. CRC Press, 2015. doi: 10.1201/b19493.

[35] L. Skedung, M. Arvidsson, J. Y. Chung, C. M. Stafford, B. Berglund, and M. W. Rutland, "Feeling Small: Exploring the Tactile Perception Limits," *Sci. Rep.*, vol. 3, no. 1, p. 2617, Sep. 2013, doi: 10.1038/srep02617.

[36] T. Yoshioka, S. J. Bensmaïa, J. C. Craig, and S. S. Hsiao, "Texture perception through direct and indirect touch: An analysis of perceptual space for tactile textures in two modes of exploration," *Somatosens. Mot. Res.*, vol. 24, no. 1–2, pp. 53–70, Jan. 2007, doi: 10.1080/08990220701318163.

[37] M. Hollins, S. Bensmaïa, K. Karlof, and F. Young, "Individual differences in perceptual space for tactile textures: Evidence from multidimensional scaling," *Percept. Psychophys.*, vol. 62, no. 8, pp. 1534–1544, Dec. 2000, doi: 10.3758/BF03212154.

[38] J. Faucheu, B. Weiland, M. Juganaru-Mathieu, A. Witt, and P.-H. Cornuault, "Tactile aesthetics: Textures that we like or hate to touch," *Acta Psychol. (Amst.)*, vol. 201, p. 102950, Oct. 2019, doi: 10.1016/j.actpsy.2019.102950.

[39] E. Bertaux, M. Lewandowski, and S. Derler, "Relationship between Friction and Tactile Properties for Woven and Knitted Fabrics," *Text. Res. J.*, vol. 77, no. 6, pp. 387–396, Jun. 2007, doi: 10.1177/0040517507074165.

[40] W. M. Bergmann Tiest and A. M. L. Kappers, "Analysis of haptic perception of materials by multidimensional scaling and physical measurements of roughness and compressibility," *Acta Psychol. (Amst.)*, vol. 121, no. 1, pp. 1–20, Jan. 2006, doi: 10.1016/j.actpsy.2005.04.005.

[41] E. AliAbbasi, V. Aydingul, A. Sezgin, U. Er, S. Turkuz, and C. Basdogan, "Tactile Perception of Coated Smooth Surfaces," *IEEE Trans. Haptics*, pp. 1–7, 2023, doi: 10.1109/TOH.2023.3274352.

[42] D. Atkinson *et al.*, "Tactile perceptions of digital textiles: a design research approach", doi: https://doi.org/10.1145/2470654.2466221.

[43] M. Peruzzini, M. Mengoni, and L. Cavalieri, “A multimodal tactile interface for immersive virtual experience,” *Int. J. Intelligent Engineering Informatics*, doi: https://doi.org/10.1504/IJIEI.2017.082563.